

Positron interactions with high- Z atoms at relativistic energies

M. N. Butler,* M.-C. Chu,[†] S. E. Koonin, and J. Piekarewicz[‡]

W. K. Kellogg Radiation Laboratory, California Institute of Technology, Pasadena, California 91125

(Received 22 March 1988)

We consider the interaction of a positron with a bound electron of a high- Z atom. In particular, we present relativistic calculations of the cross sections for knockout and/or positronium formation in a thorium target, as well as an internal process in a hypothetical $Z = 164$ "atom." Both plane-wave and distorted-wave Born approximations are discussed. We find peaks in the final sum energy of the electron-positron pairs due to the momentum distribution of the atomic electron. However, these peaks are too low in energy and are too broad compared with peaks claimed in e^+e^- scattering or with the anomalous positron peaks in heavy-ion experiments.

I. INTRODUCTION

Among the most exciting recent developments in nuclear physics is the experimental evidence for anomalous positron peaks, later found to be coincident with electrons in heavy-ion collisions close to the Coulomb barrier.¹ The positrons and electrons appear to emerge with equal kinetic energies of several hundred keV. There have been numerous attempts to explain these peaks,^{2,3} but so far none with any success.

In a related experiment, Erb and collaborators found an electron-positron coincidence peak in the final state when positrons are scattered from thorium, but no peak when a tantalum target was used.⁴ If these peaks are real (Ref. 4 states that they might be due to Compton scattering in the detectors) then it is interesting that the singles (electron or positron) peaks are at about 850 keV, which are the energies seen in the heavy-ion collision experiments.⁵

The final electron and positron kinetic energies in both cases are large enough so that processes associated with the bulk (i.e., solid-state) structure of the target can be ruled out, but atomic or nuclear phenomena cannot. The presence of an electron coincident with the positron in the final state suggests, but does not imply, an atomic process. However, the interaction of high-energy positrons with heavy atoms has not been a topic of great interest to date, perhaps because monochromatic beams have not been available and new phenomena are not obviously present.

In this paper we consider conventional atomic processes in which an incident positron knocks out a deeply bound electron (K or L shell) from a heavy atom. We have in mind here the secondary interaction of positrons produced in a heavy-ion collision with other atoms in the target or the primary interactions of the positrons in the experiment of Erb *et al.* It is not implausible that such a mechanism could produce equal-energy electron-positron pairs at a particular total energy. The Coulomb attraction between the outgoing electron and positron tends to correlate their momenta, the extreme limit being a bound state of positronium (subsequently dissociated by its passage through the target). Peaking in the total energy

arises from the momentum content of the bound-state wave function. For example, the K -shell wave function is largest at zero momentum, implying that the knockout or positronium cross section will peak at a particular incident positron (and hence total) energy. Of course, the effects of phase-space factors, being off-mass shell, and distortion of the initial and final states by the atomic potential will modify this peak. Our calculations in this paper are aimed at determining whether the locations, strengths, and widths of these peaks are at all compatible with the experiments we have cited above.

There have also been speculations that long-lived compound nuclei might be formed in heavy-ion collisions just above the Coulomb barrier.³ With this in mind, we have also considered the interaction of a positron emitted from such a system (by an unspecified mechanism) with the bound electrons. Considerations similar to those described above lead to a similar expectation of peaking in the "internal" knockout and positronium probabilities.

Our presentation is organized as follows. Section II describes nonrelativistic and relativistic plane-wave Born-approximation calculations of both the knockout and positronium formation processes induced by a mildly relativistic positron incident on a heavy atom. Section III extends the calculation to the distorted-wave Born approximation to include the effects of the atomic potential on the initial and final states. Section IV discusses internal scattering of a positron from the bound electrons of a hypothetical $Z = 164$ compound nucleus. We then draw together these three sets of results in Sec. V and discuss their relations to experimental data, before we summarize and conclude in Sec. VI.

II. PLANE-WAVE APPROXIMATION

Our plane-wave calculation is very similar to that for free Bhabha scattering,^{6,7} except that the electron is bound in the initial state. This means a fixed energy but arbitrary momentum, and the cross section will be proportional to the square of the bound-state wave function at the relevant momentum transfer. We first present a nonrelativistic plane-wave calculation to illustrate the relevant physics.

A. Nonrelativistic calculation

The initial state consists of a bound electron with wave function ψ_B , and an incident positron plane wave,

$$\psi_{\text{initial}} = \psi_B(\mathbf{r}_-) e^{i\mathbf{p}_i \cdot \mathbf{r}_+},$$

where \mathbf{p}_i is the three-momentum of the incident positron and \mathbf{r}_- (\mathbf{r}_+) is the position of the electron (positron). The final state can be written as the product of two plane waves and the relative wave function between the final positron and electron ψ_c ,

$$\psi_{\text{final}} = e^{i\mathbf{p}_+ \cdot \mathbf{r}_+} e^{i\mathbf{p}_- \cdot \mathbf{r}_-} \psi_c(\mathbf{r}_+ - \mathbf{r}_-).$$

Here \mathbf{p}_+ (\mathbf{p}_-) is the three momentum of the outgoing positron (electron). The first Born approximation to the knockout amplitude is therefore

$$M = \int d^3\mathbf{r}_+ \int d^3\mathbf{r}_- e^{-i\mathbf{p}_+ \cdot \mathbf{r}_+} e^{-i\mathbf{p}_- \cdot \mathbf{r}_-} \psi_c^*(\mathbf{r}_+ - \mathbf{r}_-) \times \frac{-e^2}{|\mathbf{r}_+ - \mathbf{r}_-|} e^{i\mathbf{p}_i \cdot \mathbf{r}_+} \psi_B(\mathbf{r}_-).$$

For small relative momenta of the electron and positron, ψ_c varies on a length scale (\AA) much greater than those of the other terms (fm) in the amplitude, while for large relative momenta $\psi_c \approx 1$. Thus we can safely put $\psi_c(r) \approx \psi_c(0)$ and move it outside of the integral. After

some straightforward manipulations and inserting the phase-space factors, we arrive at the differential cross section

$$\frac{d^3\sigma}{d\Omega_+ d\Omega_- dE_+} = \frac{\alpha^2}{2\pi^3} \frac{E_i}{p_i} \frac{p_+ p_- E_+ E_-}{(\mathbf{p}_i - \mathbf{p}_+)^4} (2j_B + 1) \times |\psi_c(0)|^2 |\psi_B(\mathbf{p}_B)|^2. \quad (1)$$

Here $\Omega_{(+,-)}$ and $E_{(+,-)}$ are the solid angles and energies for the final positron and electron, $\mathbf{p}_B = \mathbf{p}_+ + \mathbf{p}_- - \mathbf{p}_i$, and j_B is the angular momentum of the bound state. For a 1S electron, the bound wave function ψ_B peaks at zero momentum, so that the cross section will peak for nonzero momenta of the final-state pair, depending strongly upon the momentum of the incident positron. Correlations due to the final-state Coulomb attraction between the electron and positron can be accounted for by the nonrelativistic Gamow factor,

$$|\psi_c(0)|^2 \equiv f(|\mathbf{p}_+ - \mathbf{p}_-|) = \frac{2\pi\eta}{1 - e^{-2\pi\eta}}, \quad \eta = \frac{m\alpha}{|\mathbf{p}_+ - \mathbf{p}_-|} \quad (2)$$

since it is important only for small relative momenta.

We can integrate Eq. (1) over the solid angles to obtain the total cross section,

$$\frac{d\sigma}{dE_+} = \frac{\alpha^2}{\pi^2} \frac{E_i}{p_i} p_+ p_- E_+ E_- \int_{-1}^1 d\cos\theta_+ \int_{-1}^1 d\cos\theta_- \int_0^{2\pi} d\phi_- \frac{1}{(\mathbf{p}_i - \mathbf{p}_+)^4} |\psi_c(0)|^2 |\psi_B(\mathbf{p}_B)|^2, \quad (3)$$

where

$$p_B^2 = p_+^2 + p_-^2 + 2p_+ p_- (\cos\theta_+ \cos\theta_- + \sin\theta_+ \sin\theta_- \cos\phi_-) + p_i^2 - 2p_i (p_+ \cos\theta_+ + p_- \cos\theta_-),$$

and θ_{\pm} (ϕ_{\pm}) is the polar (azimuthal) angles of the final positron and electron.

The cross sections for positronium formation are very similar to Eqs. (1) and (3), except that in the phase-space factor they are modified and ψ_c is the 1s positronium wave function. Thus

$$\left[\frac{d\sigma}{d\Omega_+} \right]_{\text{Ps}} = (2\pi)^3 \frac{1}{p_+ E_+} |\psi_{\text{Ps}}(0)|^2 \left[\frac{d\sigma}{d\Omega_+ d\Omega_- dE_+} \right]_{\text{ko}} (E_+ = E_-, \theta_+ = \theta_-, \phi_- = 0).$$

Here E_+ is one half of the positronium energy, and we use the nonrelativistic positronium wave function $|\psi_{\text{Ps}}(0)|^2 = m^3 \alpha^3 / 8\pi$.

B. Relativistic calculation

The relativistic plane-wave calculation follows the same spirit as the nonrelativistic one. We must calculate the matrix element for the sum of two Feynman diagrams; scattering and annihilation (Fig. 1). The resulting cross section for knockout is given by (see Appendix A)

$$\frac{d^3\sigma}{d\Omega_+ d\Omega_- dE_+} = \frac{\alpha^2}{2\pi^3} \frac{p_+ p_-}{p_i} (2j_B + 1) |\mathcal{M}_B|^2, \quad (4)$$

$$|\mathcal{M}_B|^2 = \left[\begin{aligned} &[(k_+ \cdot k_-)(B_v \cdot k_i) + (k_- \cdot k_i)(k_+ \cdot B_v) - m^2(k_- \cdot B_v) - mB_s(k_+ \cdot k_i) + 2m^3B_s] \frac{1}{(k_i - k_+)^4} \\ &+ [(k_+ \cdot k_i)(B_v \cdot k_-) + (k_- \cdot k_i)(k_+ \cdot B_v) + m^2(k_i \cdot B_v) + mB_s(k_+ \cdot k_-) + 2m^3B_s] \frac{1}{(k_- + k_+)^4} \\ &+ [2(k_- \cdot k_i)(B_v \cdot k_+) - mB_s(k_+ \cdot k_i - k_+ \cdot k_- - k_- \cdot k_i) \\ &\quad - m^2(k_- \cdot B_v - k_+ \cdot B_v - k_i \cdot B_v) + 2m^3B_s] \frac{1}{(k_i - k_+)^2 (k_- + k_+)^2} \end{aligned} \right],$$

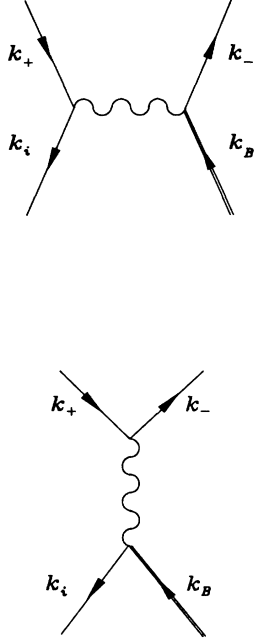


FIG. 1. First-order diagrams for a positron interacting with a bound state electron (indicated by double line).

where

$$B_v = (B_v^0, \text{sgn}(\kappa_B) F_B(p_B) G_B(p_B) \hat{\mathbf{p}}_B),$$

$$B_v^0 = \frac{[G_B^2(p_B) + F_B^2(p_B)]}{2}, \quad B_s = \frac{[G_B^2(p_B) - F_B^2(p_B)]}{2}.$$

B labels the bound-state quantum numbers, k_i , k_+ , and k_- are the four-momenta of the initial positron and final-state positron and electron, respectively [$k = (E, \mathbf{p})$]. G_B and F_B are the radial parts of the upper and lower components of the bound-state electron in momentum space, as given in Appendix A.

To study positronium formation, the cross section is modified by the phase-space restriction $\mathbf{p}_+ = \mathbf{p}_-$. The result is

$$\frac{d\sigma}{d\Omega_+} = \alpha^2 \frac{p_-}{p_i E_+} (2j_B + 1) |\mathcal{M}_B(\mathbf{p}_+ = \mathbf{p}_-)|^2 |\psi_{\text{Ps}}(0)|^2. \quad (5)$$

Note the different kinematic prefactors from the knockout cross section. The extra factor of α^3 in the positronium wave function severely reduces the magnitude of the cross section compared to the simple knockout.

III. DISTORTED-WAVE CALCULATION

Since the potential energy at the K shell of thorium ($Z=90$) is about 200 keV, we expect a significant Coulomb distortion of the incident and outgoing particles in the scattering process. Indeed, a naive treatment of this distortion using the appropriate Gamow factors shows that the cross section will be dramatically different in the distorted case. A relativistic treatment taking into account the Coulomb distortion of the electron and posi-

tron wave functions is therefore in order.

We approach the problem using the relativistic distorted-wave Born approximation, which consists of evaluating the graphs in Fig. 1, but replacing the lepton plane-wave states by distorted waves. In this case, the electron and positron spinors, as well as the photon propagator, are expanded in partial waves, and the amplitudes are calculated explicitly before adding and squaring to give the cross section. The differential cross section for electron-positron knockout is given by

$$\begin{aligned} \frac{d^3\sigma}{dE_+ d\Omega_+ d\Omega_-} &= \frac{1}{(2\pi)^5} \frac{E_i}{p_i} (p_+ E_+ p_- E_-) \\ &\times f(|\mathbf{p}_+ - \mathbf{p}_-|) \\ &\times \frac{1}{2} \sum_{S,P,Q,M_Q} |\mathcal{M}(S,P,Q,M_Q;\kappa_B)|^2, \end{aligned} \quad (6)$$

where $f(|\mathbf{p}_+ - \mathbf{p}_-|)$ is a correlation function describing the final-state interaction of the emerging leptons. In the case of positronium formation, the differential cross section is

$$\begin{aligned} \left[\frac{d\sigma}{d\Omega_+} \right]_{\text{Ps}} &= \frac{1}{(2\pi)^2} \frac{E_i}{p_i} \left[\frac{p_+ E_+}{2} \right] |\psi_{\text{Ps}}(0)|^2 \\ &\times \frac{1}{2} \sum_{\substack{S,P \\ Q,M_Q}} |\mathcal{M}(S,P,Q,M_Q;\kappa_B)|^2_{\mathbf{p}_+ = \mathbf{p}_-}, \end{aligned} \quad (7)$$

where $E_+ = (E_i + E_B)/2$, and the positronium wave function has been evaluated at the origin. We can integrate the cross sections over the solid angles Ω_+ and Ω_- to obtain the total knockout cross section. The outline of the calculation of the matrix elements \mathcal{M} and the final cross-section formulas are given in Appendix B.

As a test of our distorted-wave calculation, we examined the convergence of the cross section as a function of the number of partial waves. The convergence of the total cross section with the partial-wave sum is quite rapid; four partial waves in the photon propagator and eight in the lepton wave functions were sufficient for convergence to 10% accuracy. We also find that the cross section with the distortions omitted is in good agreement with the plane-wave results of the previous section. However, the convergence of the angle-differential cross section with partial waves is quite slow. Cross terms between different partial waves are important here and so the contributions of higher partial waves are amplified when they interfere with lower partial waves. Because of practical limits on the number of partial waves we can include in our calculations, we will not present results for angle-differential cross sections in this paper.

IV. INTERNAL SCATTERING WHEN $Z = 164$

Reinhardt *et al.*³ have proposed that a compound nucleus might be formed during heavy-ion collisions at energies just above the Coulomb barrier. Such a compound nucleus would have an "atomic" charge so large that the electric fields around it would be very high. In fact, for

supercritical systems ($Z \geq 173$), it is expected that the vacuum will break down spontaneously, producing electron-positron pairs.³ We discuss in this section the scattering of a positron produced close to a hypothetical $Z=164$ compound nucleus with one of its bound-state electrons.

The first-order diagrams we need to evaluate are the same as those in Fig. 1, except that now a Coulomb distorted propagator

$$S_p(\mathbf{R}, \mathbf{r}_1) = i\pi \sum_{\kappa_i, \mu} \psi_{\kappa_i, \mu}(\mathbf{R}) \bar{\psi}_{\kappa_i, \mu}^{(+)}(\mathbf{r}_1) \quad (8)$$

is used for the incident positron, instead of a distorted-wave spinor. In Eq. (8), the propagator is formed from the Coulomb distorted positron wave functions $\psi_{\kappa_i, \mu}^{(+)}$, with outgoing waves boundary conditions. We have specified that the positron propagates from coordinate $\mathbf{R} \approx \mathbf{0}$ (close to the nucleus) to \mathbf{r}_1 , but not the physical process that produces the positron. Then the contribution from higher partial waves in the sum in Eq. (8) is small, and we can approximate the propagator by its S -wave component only,

$$\psi_{-1\mu}^{(+)}(\mathbf{r}_1) = \left[\frac{E_i + m}{\pi} \right]^{1/2} \sqrt{p_i} \frac{1}{p_i r_1} \times \begin{bmatrix} -i\mathcal{I}(r_1) | (1 \frac{1}{2}) \frac{1}{2}, -\mu \rangle \\ \mathcal{G}(r_1) | (0 \frac{1}{2}) \frac{1}{2}, -\mu \rangle \end{bmatrix},$$

where

$$\mathcal{G}(r_1) = i\mathcal{R} + \mathcal{I} \rightarrow p_i r_1 h_0(p_i r_1) \rightarrow e^{i(p_i r_1 + \delta_i)}$$

at asymptotically large r_1 . Here \mathcal{R} and \mathcal{I} are the regular and irregular solutions, respectively, of the Dirac equation with a Lenz-Jensen potential (defined in Appendix B) and $p_i = (E_i^2 - m^2)^{1/2}$.

The absolute cross section of internal scattering depends on the particular process that creates the positron. However, we are interested only in the ratio of the internal scattering cross section to the cross section of a positron being emitted without interacting with the electrons. To study a simple example, we assume that the coupling between the positron and its source has the form $g\psi_x\gamma_0\psi_+$, where ψ_+ is the wave function of the emitted positron and ψ_x is arbitrary and will factor out when we take the ratio. The rest of the calculation is now very similar to that in Sec. III, except that for such a high- Z system, the bound-state wave functions would be drawn very close to the nucleus, and we can no longer use the hydrogen atom wave functions for the bound state electrons. We instead integrate the Dirac equation with a smeared nuclear charge and obtain the bound-state wave functions numerically. The rate of positron internal scattering is

$$\frac{d\Gamma}{dE_+} = \frac{p_i^2}{2} \left[\frac{d\sigma}{dE_+} \right]_{\text{ext}}, \quad (9)$$

where $\Gamma = R_s/R_f$ is the ratio of the rates of internal scattering events to free positron emission. $(d\sigma/dE_+)_{\text{ext}}$ is the differential cross section for scattering using the formula for external scattering, Eq. (B8),

but with the positron propagator replacing the incident wave function.

V. RESULTS

If thick targets are used (such as the one of Erb *et al.*), $\approx 50 \text{ mg/cm}^2$, electrons and positrons undergo multiple scattering in the target sufficient to destroy any angular information, so that we need consider only the total cross sections for knockout. The plane-wave calculation is straightforward, with good convergence in the angular integrals using 48-point Gauss-Legendre quadrature (needed for convergence at high E). The distorted-wave calculation was performed on the National Science Foundation-San Diego Supercomputer Center (NSF/SDSC) Cray X-MP computer and convergence was good, as discussed in Sec. III. The calculation took about 5 central-processing-unit (CPU) minutes per point in the $E_+ - E_-$ plane.

In Figs. 2(a) and 2(b) we show the total cross section for knockout of a $1S$ electron in $_{90}\text{Th}$ without and with distortion. Both cases are Bhabha-like, with a large cross

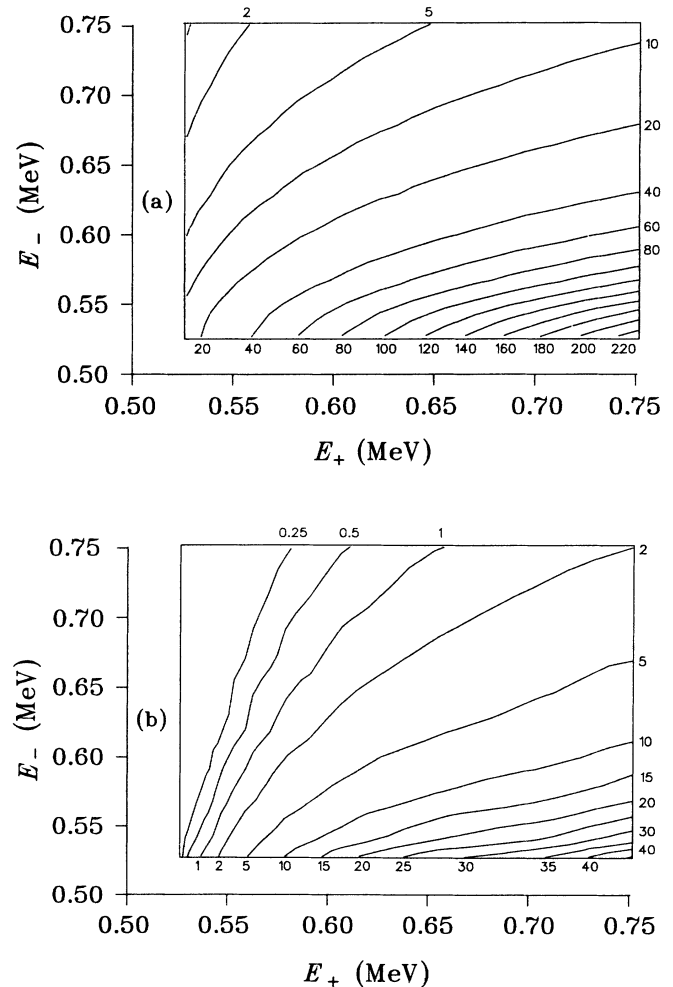


FIG. 2. Angle-integrated knockout cross section (barn/MeV) for positron scattering from the $1S$ electrons of a thorium atom. The final electron (E_-) and positron energy (E_+) are in MeV. The plane-wave (a) and distorted-wave (b) results are shown.

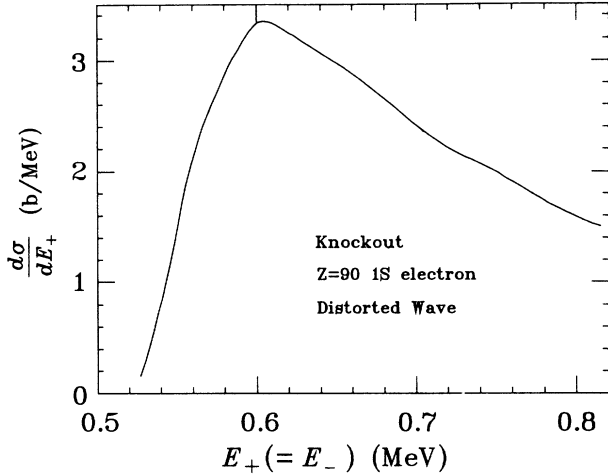


FIG. 3. The cross section in Fig. 2(b) along the $E_+ = E_-$ diagonal.

section at high-positron and low-electron energies. There is a broad hump at low energies reflecting the momentum distribution of the bound-state electrons. This is shown clearly in Fig. 3, where the distorted-wave cross section is plotted along the $E_+ = E_-$ diagonal. Comparing the plane-wave and distorted-wave results, we find that the distortion pushes the peak to higher energy, although only by about 50 keV. This peak in the sum energy is too low and too broad compared to those seen in either the Gesellschaft für Schwerionenforschung Darmstadt (GSI) or Erb's experiments. Knockout from higher shells gives narrower sum peaks, but at even lower energies (see Table I). We found no peaks in the difference spectrum, as angle integration destroys the final-state Coulomb correlation.

In Fig. 4 we show the cross section for positronium formation from a 1S electron of $_{90}\text{Th}$ as a function of the final positron energy (half of the positronium energy). Again comparing with the plane-wave results, we find that distortion suppresses the cross section, as well as pushing the peak to a higher energy. The sum peak is quite narrow, though again at too low an energy when compared with experiments. Results for higher shells are qualitatively similar (Table I). A comparison of Figs. 3 and 4 shows that positronium formation is suppressed by a factor of 10^6 relative to knockout.

The internal scattering cross section for 1S knockout and positronium formation in a $Z = 164$ compound nucleus are shown in Fig. 5. The sum peaks move up to 0.88 and 1.25 MeV, respectively, but are very broad

TABLE I. Location and widths of peaks in the cross section for external positron scattering from thorium. Widths are given at half maximum.

Electron states	Knockout (MeV)	Positronium (MeV)
1S	$0.61_{-0.06}^{+0.18}$	$0.58_{-0.04}^{+0.10}$
2S	$0.54_{-0.02}^{+0.03}$	$0.53_{-0.01}^{+0.02}$
$2P_{1/2}$	$0.54_{-0.02}^{+0.04}$	$0.54_{-0.02}^{+0.03}$

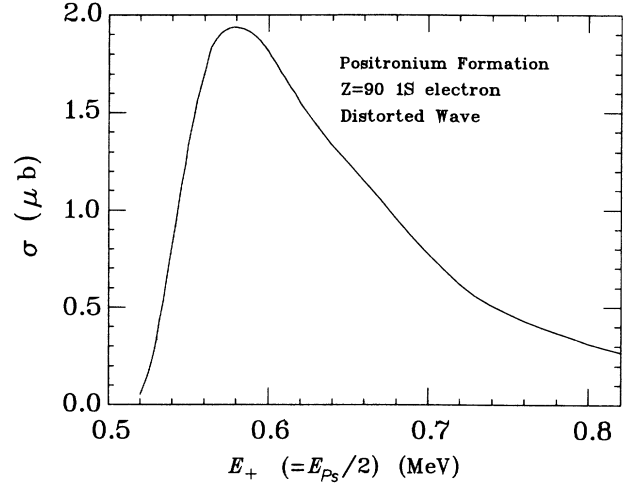


FIG. 4. Positronium formation cross section with 1S thorium electrons, as a function of half of the positronium energy.

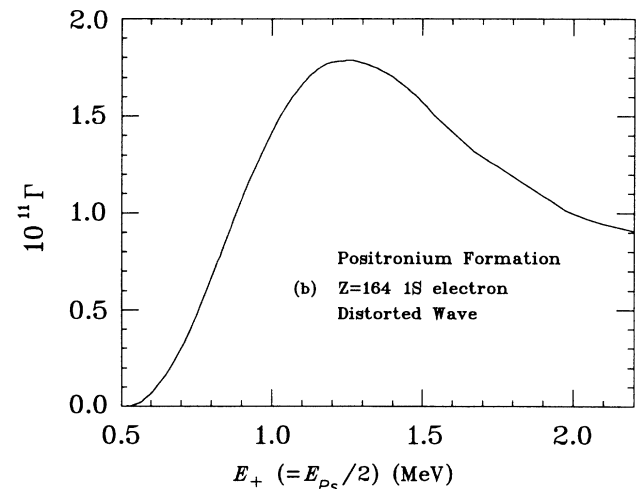
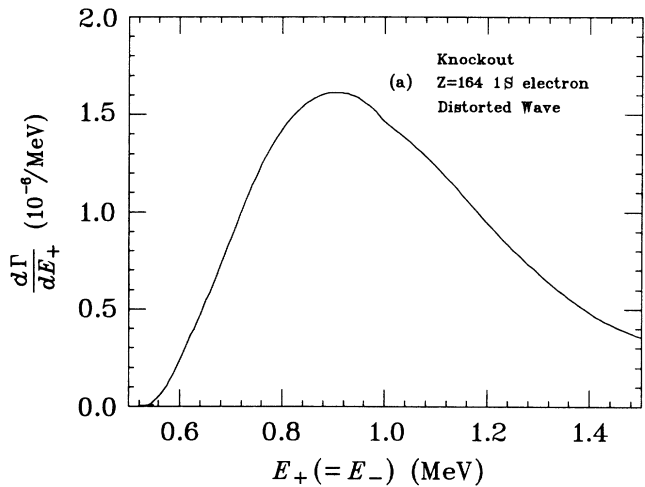


FIG. 5. Ratio of the rates of internal positron scattering and free positron emission in a hypothetical $Z = 164$ "atom," for (a) knockout and (b) positronium formation.

TABLE II. Location and widths of peaks in the cross section for internal positron scattering in a $Z = 164$ atom. Widths are given at half maximum.

Electron states	Knockout (MeV)	Positronium (MeV)
1S	$0.88_{-0.20}^{+0.36}$	$1.25_{-0.40}^{+0.95}$
2S	$0.77_{-0.14}^{+0.26}$	$0.85_{-0.20}^{+0.70}$
$2P_{1/2}$	$0.87_{-0.22}^{+0.50}$	$1.0_{-0.3}^{+1.2}$
$2P_{3/2}$	$0.61_{-0.06}^{+0.11}$	$0.66_{-0.09}^{+0.32}$
3S	$0.61_{-0.05}^{+0.10}$	$0.61_{-0.05}^{+0.16}$

(≈ 0.5 – 1.0 MeV); these can both be understood as consequences of a more deeply bound electron with a broader momentum distribution. Results from higher shells are again qualitatively similar (Table II).

VI. SUMMARY AND CONCLUSION

We have shown that positron knockout of a bound-state electron in a high- Z atom gives rise to peak structures in the final sum energy of the electron-positron pair. For external scattering by a thorium target, we found that the peaks corresponding to the knockout from inner shells are all at relatively low energies, $E_{\text{sum}} \leq 1.2$ MeV. Distortion of the lepton waves moves the peaks to slightly higher energies relative to a plane-wave calculation, but at the same time suppresses the cross section. The knockout cross sections show no peak structures in the difference energy spectrum, and positronium formation cross section is suppressed by a factor of $\approx \alpha^3$ compared to knockout. Internal scattering of a positron in a $Z = 164$ atom also shows peaks in the final sum energy. These peaks are at much higher energies ($E_{\text{sum}} \approx 1.7$ – 2.5 MeV) than those for thorium, though their widths are also much larger. In conclusion, the atomic processes we have considered in this paper do not seem to be directly responsible for either the Erb's peak or the GSI peaks.

ACKNOWLEDGMENTS

We would like to thank Dr. V. Pönisch and Dr. A. Schäfer for useful discussions. One of us (M.-C.C.)

thanks the Institut für Theoretische Physik der Universität Frankfurt for their hospitality and Dr. T. Elze for helpful discussions. Most of the numerical computation was done on the NSF/SDSC Cray X-MP computer; the assistance of the San Diego Supercomputer Center is appreciated. This work is supported partially by NSF Grant Nos. PHY-86-04197 and PHY-85-05682. One of us (M.N.B.) is grateful for financial support of the Natural Sciences and Engineering Research Council of Canada.

APPENDIX A: PLANE-WAVE-CALCULATION DETAILS

In this appendix we derive the plane-wave amplitude for the knockout of a bound electron by an incident positron. We will follow the conventions of Bjorken and Drell.⁷ The transition-matrix element is given by the difference of the direct and annihilation terms,

$$\mathcal{M}_B = e^2 \left[\bar{v}(k_i) \gamma_\mu v(k_+) \frac{1}{(k_+ - k_i)^2} \bar{u}(k_-) \gamma^\mu u_B(k_B) - \bar{u}(k_-) \gamma_\mu v(k_+) \frac{1}{(k_i + k_B)^2} \bar{v}(k_i) \gamma^\mu u_B(k_B) \right].$$

The only difference between this matrix element and that of Bhabha scattering is that the initial electron is in a bound state

$$u_B = \begin{bmatrix} G_B \\ -\text{sgn}(\kappa_B) \sigma \cdot \hat{\mathbf{p}}_B F_B \end{bmatrix} \mathcal{Y}_{j_B l_B \frac{1}{2}}^M,$$

with σ the Pauli spin matrices and \mathcal{Y} a spin-angular harmonic. G_B and F_B are the radial parts of the upper and lower components of the wave function in momentum space. For scattering from electrons in the inner shells of thorium ($Z = 90$), we use hydrogen wave functions. For example, for the 1S state,

$$G_B(p_B) = C_1 \frac{4\pi}{p_B} \frac{\Gamma(\gamma+1)}{(a^2 + p_B^2)^{(\gamma+1)/2}} \times \sin \left[(\gamma+1) \tan^{-1} \left(\frac{p_B}{a} \right) \right]$$

and

$$F_B(p_B) = 4\pi C_2 \left\{ \frac{\Gamma(\gamma)}{p_B} \frac{1}{(p_B^2 + a^2)^{\gamma/2}} \sin \left[\gamma \tan^{-1} \left(\frac{p_B}{a} \right) \right] - \frac{\Gamma(\gamma+1)}{p_B} \frac{1}{(p_B^2 + a^2)^{(\gamma+1)/2}} \cos \left[(\gamma+1) \tan^{-1} \left(\frac{p_B}{a} \right) \right] \right\},$$

where

$$C_1 = \frac{(2a)^{\gamma+1/2}}{\sqrt{4\pi}} \left[\frac{1+\gamma}{2\Gamma(1+2\gamma)} \right]^{1/2},$$

and $C_2 = [(\gamma-1)/Z\alpha] C_1$. We have defined $\gamma \equiv (1 - Z^2\alpha^2)^{1/2}$ and $a \equiv mZ\alpha$.

We can evaluate $u_B \bar{u}_B$ explicitly as

$$u_B \bar{u}_B = \frac{(2j_B+1)}{8\pi} (B_s + \gamma \cdot B_v),$$

where B_s and B_v are defined in Eq. (4). We can therefore calculate the square of the matrix element (summed over final spins and initial electron spins, averaged over initial positron spins), using standard trace techniques.⁷ The result is given in Eq. (4).

APPENDIX B: DISTORTED-WAVE CALCULATION DETAILS

In this appendix we derive the distorted-wave amplitude for the knockout of a bound electron by an incident

positron. The transition amplitude is given by the difference of the direct and annihilation terms,

$$T_d = \int d^4x \int d^4y [\bar{u}_{k_-s_-}^{(-)}(x)(-ie\gamma^\mu)u_B(x)]iD_{\mu\nu}(x,y) \\ \times [\bar{v}_{k_+s_+}^{(+)}(y)(-ie\gamma^\nu)v_{k_+s_+}^{(-)}(y)] ,$$

$$T_a = \int d^4x \int d^4y [\bar{u}_{k_-s_-}^{(-)}(x)(-ie\gamma^\mu)v_{k_+s_+}^{(-)}(x)] \\ \times iD_{\mu\nu}(x,y)[\bar{v}_{k_+s_+}^{(+)}(y)(-ie\gamma^\nu)u_B(y)] ,$$

where

$$iD_{\mu\nu}(x,y) = \int \frac{d^4q}{(2\pi)^4} e^{-iq \cdot (x-y)} \frac{-ig_{\mu\nu}}{q^2 + i\epsilon}$$

is the photon propagator, u and v are distorted wave spinors related by charge conjugation,

$$v_{ks}^{(\pm)}(x) = i\gamma^2 u_{ks}^{(\mp)*}(x) ,$$

and displaying the appropriate boundary conditions. In the presence of the strong Coulomb field generated by the heavy nucleus, the Dirac spinors do not satisfy the free Dirac equation and therefore no longer carry a simple plane-wave dependence. The spinors, however, still carry a simple harmonic time dependence, which enables us to perform both time integrals, as well as the integral involving the photon propagator, in a straightforward way. The transition amplitude can thus be written as

$$T = -2\pi i \delta(E_i + E_B - E_+ - E_-) \mathcal{M} ,$$

where $\mathcal{M} = \mathcal{M}_d - \mathcal{M}_a$, with

$$\mathcal{M}_d = \left[\frac{e^2}{4\pi} \right] \int d^3\mathbf{x} \int d^3\mathbf{y} [\bar{u}_{p_-s_-}^{(-)}(\mathbf{x})\gamma^\mu u_B(\mathbf{x})] \frac{e^{it|\mathbf{x}-\mathbf{y}|}}{|\mathbf{x}-\mathbf{y}|} \\ \times [\bar{v}_{p_+s_+}^{(+)}(\mathbf{y})\gamma_\mu v_{p_+s_+}^{(-)}(\mathbf{y})] , \quad (\text{B1a})$$

$$v_{ps}^{(\pm)}(\mathbf{x}) = \left[\frac{E+m}{2E} \right]^{1/2} \sum_{\kappa, M, m_l} 4\pi i^l (-1)^{j-M} \langle l m_l; \frac{1}{2} m_s | j M \rangle e^{\pm i\delta_l(p)} \frac{Y_{lm_l}(\hat{\mathbf{p}})}{px} \begin{bmatrix} -iF_{E\kappa}(x) \langle \hat{\mathbf{x}} | -\kappa, -M \rangle \\ G_{E\kappa}(x) \langle \hat{\mathbf{x}} | \kappa, -M \rangle \end{bmatrix} . \quad (\text{B2b})$$

In the preceding expressions, $E = (p^2 + m^2)^{1/2}$ is the energy of the lepton and the spinors have been normalized to one particle per unit volume. The radial components of the Dirac spinors are real functions of x satisfying the first-order coupled differential equations

$$\left[\frac{d}{dx} + \frac{\kappa}{x} \right] G_{E\kappa}(x) = [E + m - V(x)] F_{E\kappa}(x) , \quad (\text{B3a})$$

$$\left[\frac{d}{dx} - \frac{\kappa}{x} \right] F_{E\kappa}(x) = -[E - m - V(x)] G_{E\kappa}(x) , \quad (\text{B3b})$$

with boundary conditions to be specified below, and with a relative minus sign between the electron-nucleus and positron-nucleus potentials.

The preceding system of differential equations can be

$$\mathcal{M}_a = \left[\frac{e^2}{4\pi} \right] \int d^3\mathbf{x} \int d^3\mathbf{y} [\bar{u}_{p_-s_-}^{(-)}(\mathbf{x})\gamma^\mu v_{k_+s_+}^{(-)}(\mathbf{x})] \\ \times \frac{e^{is|\mathbf{x}-\mathbf{y}|}}{|\mathbf{x}-\mathbf{y}|} [\bar{v}_{p_+s_+}^{(+)}(\mathbf{y})\gamma_\mu u_B(\mathbf{y})] . \quad (\text{B1b})$$

$t = E_i - E_+ = E_- - E_B$ is the energy transfer to the electron and $s = E_i + E_B = E_- + E_+$ is the total energy of the pair. We evaluate the two remaining spatial integrals by performing a multipole decomposition of all Dirac spinors, as well as of the photon propagator. The angular integrals are evaluated analytically using standard techniques in angular momentum algebra, while the two remaining radial integrals must be performed numerically.

To perform the expansion of the Dirac spinors, we use spin-angular harmonics defined by

$$\langle \hat{\mathbf{x}} | \kappa M \rangle \equiv \mathcal{Y}_{j l (1/2)}^M(\hat{\mathbf{x}}) ,$$

where κ is a nonzero integer, $j = |\kappa| - \frac{1}{2}$, and

$$l = \begin{cases} \kappa & \text{if } \kappa > 0 \\ -(1+\kappa) & \text{if } \kappa < 0 \end{cases} .$$

The electron spinors can then be written as

$$u_{ps}^{(\pm)}(\mathbf{x}) = \left[\frac{E+m}{2E} \right]^{1/2} \\ \times \sum_{\kappa, M, m_l} 4\pi i^l \langle l m_l; \frac{1}{2} m_s | j M \rangle e^{\pm i\delta_l(p)} \frac{Y_{lm_l}^*(\hat{\mathbf{p}})}{px} \\ \times \begin{bmatrix} G_{E\kappa}(x) \langle \hat{\mathbf{x}} | \kappa, M \rangle \\ iF_{E\kappa}(x) \langle \hat{\mathbf{x}} | -\kappa, M \rangle \end{bmatrix} , \quad (\text{B2a})$$

while the positron spinors are simply obtained by charge conjugation,

easily manipulated into a one dimensional Schrödinger-type equation. We write the lower component of the wave function in terms of the upper,

$$F_{E\kappa}(x) = \frac{1}{[E + m - V(x)]} \left[\frac{d}{dx} + \frac{\kappa}{x} \right] G_{E\kappa}(x) ,$$

substitute it into the second equation, and introduce $\phi_{l\kappa}(x)$ through the definition

$$G_{E\kappa}(x) = \sqrt{E + m - V(x)} \phi_{l\kappa}(x)$$

to obtain

$$\left[\frac{d^2}{dx^2} + k^2 - \frac{l(l+1)}{x^2} - U(x) \right] \phi_{l\kappa}(x) = 0$$

together with the boundary conditions

$$\begin{aligned}\phi_{lk}(x=0) &= 0, \\ \phi_{lk}(x) &\sim \sin \left[kx - \frac{l\pi}{2} + \delta_l(k) \right] \quad \text{as } x \rightarrow \infty.\end{aligned}$$

The effective potential $U(x)$ is given by

$$\begin{aligned}U(x) &= 2EV(x) - V^2(x) - \frac{\kappa}{E+m-V(x)} \frac{1}{x} \frac{dV}{dx} \\ &+ \frac{3}{4(E+m-V)^2} \left[\frac{dV}{dx} \right]^2 + \frac{1}{2(E+m-V)} \frac{d^2V}{dx^2}.\end{aligned}$$

We use the Lenz-Jensen approximation to the Thomas-Fermi potential,⁸

$$V(r) = -\frac{Ze^2}{r} e^{-y(1+y+b_2y^2+b_3y^3+b_4y^4)},$$

with

$$b_2=0.3344, \quad b_3=0.0485, \quad b_4=2.647 \times 10^{-3},$$

and $y=0.20166Z^{1/6}r^{1/2}$ (r in MeV^{-1} , V in MeV).

After expanding the photon propagator in spherical harmonics, with coefficients given in terms of spherical Bessel functions,

$$\frac{e^{it|\mathbf{x}-\mathbf{y}|}}{|\mathbf{x}-\mathbf{y}|} = 4\pi t \sum_{\lambda,\mu} j_\lambda(tx_<) h_\lambda^{(+)}(tx_>) Y_{\lambda\mu}(\hat{\mathbf{x}}) Y_{\lambda\mu}^*(\hat{\mathbf{y}}),$$

where $x_> = \max\{|\mathbf{x}|, |\mathbf{y}|\}$ and $x_< = \min\{|\mathbf{x}|, |\mathbf{y}|\}$. We can evaluate analytically the angular part of the scattering amplitude. A typical matrix element encountered in the evaluation of the direct amplitude has the form

$$\begin{aligned}B &= \sum_m (-1)^{j-m} \langle \kappa_- m_- | (Y_\lambda \sigma_\nu)_{jm} | \kappa_B m_B \rangle \langle \kappa_i, -m_i | (Y_\lambda \sigma_\nu)_{j,-m} | \kappa_+, -m_+ \rangle \\ &= \sum_m (-1)^{j-m} \langle j_B m_B; j m | j_- m_- \rangle \langle j_+, -m_+; j, -m | j_i, -m_i \rangle \langle \kappa_- || (Y_\lambda \sigma_\nu)_j || \kappa_B \rangle \langle \kappa_i || (Y_\lambda \sigma_\nu)_j || \kappa_+ \rangle \\ &= \sum_{J,M} (-1)^{j_i-m_i+j_+-m_+} \hat{j}_i \hat{j}_- \langle j_i m_i; j_B m_B | JM \rangle \langle j_- m_-; j_+ m_+ | JM \rangle \begin{Bmatrix} j_B & j_- & j \\ j_+ & j_i & J \end{Bmatrix} \\ &\quad \times \langle \kappa_- || (Y_\lambda \sigma_\nu)_j || \kappa_B \rangle \langle \kappa_i || (Y_\lambda \sigma_\nu)_j || \kappa_+ \rangle,\end{aligned}$$

where the reduced matrix element is given by

$$R_{\lambda\nu j}^{\kappa_a, \kappa_b} \equiv \langle \kappa_b || (Y_\lambda \sigma_\nu)_j || \kappa_a \rangle = \frac{\hat{\frac{1}{2}} \hat{l}_a \hat{j}_a \hat{\lambda} \hat{\nu} \hat{j}}{\sqrt{4\pi}} \langle l_a 0; \lambda 0 | l_b 0 \rangle \begin{Bmatrix} l_b & l_a & \lambda \\ \frac{1}{2} & \frac{1}{2} & \nu \\ j_b & j_a & j \end{Bmatrix},$$

and $\hat{j} \equiv \sqrt{2j+1}$. Similar expressions appear in the evaluation of the annihilation term.

We simplify the calculation of the scattering cross section by changing from the jj to the LS coupling scheme. We combine the above two Clebsch-Gordan (CG) coefficients together with the CG coefficients appearing in the definition of the Dirac distorted spinors, (B2), and perform all the necessary Dirac algebra to obtain

$$\mathcal{M}(m_B, m_{s_i}, m_{s_-}, m_{s_+}) = \sum_{\substack{S, M_S, \\ P, M_P, \\ Q, M_Q}} \langle \frac{1}{2} m_{s_-}; \frac{1}{2} m_{s_+} | SM_S \rangle \langle \frac{1}{2} m_{s_i}; j_B m_B | PM_P \rangle \langle SM_S; P, -M_P | QM_Q \rangle \mathcal{M}(SPQM_Q; \kappa_B), \quad (\text{B4})$$

where

$$\begin{aligned}\mathcal{M}(S, P, Q, M_Q; \kappa_B) &= \left[\frac{e^2}{4\pi} \right] \sum_{\kappa, M, \lambda, j, L, M_L} (-1)^\Theta \mathcal{C}_{\kappa LSJPQ} R_{\lambda j \kappa} A_{l_- m_{l_-}}^{(+)}(-\mathbf{p}_-) A_{l_+ m_{l_+}}^{(-)}(\mathbf{p}_+) A_{l_i - m_{l_i}}^{(-)}(\mathbf{p}_i) \\ &\quad \times \langle l_- m_{l_-}; l_+ m_{l_+} | LM_L \rangle \langle LM_L; l_i, -m_{l_i} | Q, -M_Q \rangle,\end{aligned} \quad (\text{B5})$$

and we have defined

$$\kappa \equiv \{\kappa_i, \kappa_+, \kappa_-\}, \quad M \equiv \{m_{l_i}, m_{l_+}, m_{l_-}\},$$

$$\Theta = \lambda + S + P + \kappa_B,$$

$$\mathcal{C}_{\kappa LSJPQ} = (2j_i+1)(2j_-+1)(2J+1) \hat{j}_+ \hat{L} \hat{S} \hat{P} \begin{Bmatrix} l_i & \frac{1}{2} & j_i \\ j_B & J & P \end{Bmatrix} \begin{Bmatrix} L & S & J \\ P & l_i & Q \end{Bmatrix} \begin{Bmatrix} l_- & l_+ & L \\ \frac{1}{2} & \frac{1}{2} & S \\ j_- & j_+ & J \end{Bmatrix},$$

$$R_{\lambda j \kappa} = [I_{\lambda j \kappa}(t) + J_{\lambda j \kappa}(t) + K_{\lambda j \kappa}(s) + L_{\lambda j \kappa}(s)],$$

$$\begin{aligned}
A_{lm}^{(\pm)}(\mathbf{p}) &= 4\pi i^l \left[\frac{E+m}{2E\Omega} \right]^{1/2} e^{\pm i\delta_l(k)} \frac{Y_{lm}(\hat{\mathbf{p}})}{p}, \\
I_{\lambda J\kappa}(t) &= \mathcal{S}_\lambda R_{\lambda 0\lambda}^{\kappa_-, \kappa_B} R_{\lambda 0\lambda}^{\kappa_i, \kappa_+} \int_0^\infty dx \int_0^\infty dy W_\lambda(x, y; t) (G_- G_B + F_- F_B)(x) (G_i G_+ + F_i F_+)(y), \\
J_{\lambda J\kappa}(t) &= \sum_j \mathcal{S}_j \int_0^\infty dx \int_0^\infty dy W_\lambda(x, y; t) [(R_{\lambda 1j}^{\kappa_-, \kappa_B} G_- F_B - R_{\lambda 1j}^{\kappa_-, \kappa_B} G_B F_-)(x) \\
&\quad \times (R_{\lambda 1j}^{\kappa_i, \kappa_+} G_+ F_i - R_{\lambda 1j}^{\kappa_i, \kappa_+} G_i F_+)(y)], \\
K_{\lambda J\kappa}(s) &= \frac{\delta_{\lambda J}}{2\lambda+1} R_{\lambda 0\lambda}^{\kappa_-, \kappa_+} R_{\lambda 0\lambda}^{\kappa_i, \kappa_B} \int_0^\infty dx \int_0^\infty dy W_\lambda(x, y; s) (G_- F_+ + G_+ F_-)(x) (G_B F_i + G_i F_B)(y), \\
L_{\lambda J\kappa}(s) &= \frac{1}{2J+1} \int_0^\infty dx \int_0^\infty dy W_\lambda(x, y; s) [(R_{\lambda 1j}^{\kappa_-, \kappa_+} G_- G_+ - R_{\lambda 1j}^{\kappa_-, \kappa_+} F_- F_+)(x) \\
&\quad \times (R_{\lambda 1j}^{\kappa_i, \kappa_B} G_i G_B - R_{\lambda 1j}^{\kappa_i, \kappa_B} F_i F_B)(y)], \\
\mathcal{S}_\lambda &\equiv \begin{Bmatrix} j_+ & j_i & \lambda \\ j_B & j_- & J \end{Bmatrix}, \quad W_\lambda(x, x'; t) \equiv 4\pi t j_\lambda(tx_-) h_\lambda^{(+)}(tx_+).
\end{aligned}$$

Cross sections for the different unpolarized processes of interest can now be simply written in terms of $\mathcal{M}(S, P, Q, M_Q; \kappa_B)$. The knockout cross section is

$$\frac{d^3\sigma}{dE_+ d\Omega_+ d\Omega_-} = \frac{1}{(2\pi)^5} \left[\frac{E_i}{p_i} \right] (p_+ E_+ p_- E_-) f(|\mathbf{p}_+ - \mathbf{p}_-|)^{\frac{1}{2}} \sum_{\substack{S, P, \\ Q, M_Q}} |\mathcal{M}(SPQM_Q; \kappa_B)|^2, \quad (\text{B6})$$

where $f(|\mathbf{p}_+ - \mathbf{p}_-|)$ is a correlation function describing the final-state interaction of the emerging leptons, and $p_i = (E_i^2 - m^2)^{1/2}$, etc. In the case of positronium formation, the differential cross section is

$$\frac{d\sigma}{d\Omega_{\text{Ps}}} = \frac{1}{(2\pi)^2} \left[\frac{E_i}{p_i} \right] \left[\frac{p_+ E_+}{2} \right] |\psi_{\text{Ps}}(0)|^2 \frac{1}{2} \sum_{\substack{S, P, \\ Q, M_Q}} |\mathcal{M}(S, P, Q, M_Q; \kappa_B)|^2_{\mathbf{p}_+ = \mathbf{p}_-}, \quad (\text{B7})$$

where $E_+ = (E_i + E_B)/2$ and the positronium wave function has been evaluated at the origin.

We can integrate Eq. (B6) over the solid angles to obtain the angle-integrated knockout cross sections. We first expand the correlation function in spherical harmonics,

$$f(|\mathbf{p}_+ - \mathbf{p}_-|) = \sum_{l, m} \frac{4\pi}{2l+1} f_l(k_+, k_-) Y_{lm}(\hat{\mathbf{p}}_+) Y_{lm}^*(\hat{\mathbf{p}}_-),$$

with the coefficients given by the orthogonality of the Legendre polynomials:

$$\frac{f_l(k_+, k_-)}{2l+1} = \frac{1}{2} \int_{-1}^1 dz P_l(z) f((p_+^2 + p_-^2 - 2p_+ p_- z)^{1/2}).$$

We then do the angular integration using the relation

$$\int d\Omega_p Y_{l_1 m_{l_1}}^*(\hat{\mathbf{p}}) Y_{l_2 m_{l_2}}(\hat{\mathbf{p}}) Y_{l_3 m_{l_3}}(\hat{\mathbf{p}}) = \frac{\hat{l}_2 \hat{l}_3}{\sqrt{4\pi \hat{l}_1}} \langle l_3 m_{l_3}; l_2 m_{l_2} | l_1 m_{l_1} \rangle \langle l_3 0; l_2 0 | l_1 0 \rangle.$$

The final result for the knockout angle-integrated cross section is

$$\frac{d\sigma}{dE_+} = \frac{2\alpha^2}{p_i^2} \left[\frac{E_i + m}{p_i} \right] \left[\frac{E_+ + m}{p_+} \right] \left[\frac{E_- + m}{p_-} \right] |M_{\text{ko}}|^2, \quad (\text{B8})$$

with

$$\begin{aligned}
|M_{\text{ko}}|^2 &= \sum_{S, P, Q} (2Q+1) \sum_{\substack{\{\kappa\}, \lambda, J, \\ \{\kappa'\}, \lambda', J', \\ L, L'}} \delta_{LL'} \delta_{l_l l_l'} (-1)^{\lambda} \phi(l_+, l_-) \mathcal{C}_{\kappa L S J P Q} R_{\lambda J \kappa} \hat{l}_+ \hat{l}_- \\
&\quad \times (-1)^{\lambda'} \phi^*(l'_+, l'_-) \mathcal{C}_{\kappa' L' S' J' P' Q'} R_{\lambda' J' \kappa'}^* \hat{l}'_+ \hat{l}'_- (-1)^{l'+L} \\
&\quad \times \frac{f_l(k_+, k_-)}{2l+1} \begin{Bmatrix} l'_- & l_- & l \\ l_+ & l'_+ & L \end{Bmatrix} \langle l_+ 0; l'_+ 0 | l 0 \rangle \langle l_- 0; l'_- 0 | l 0 \rangle, \quad (\text{B9})
\end{aligned}$$

where

$$\phi(l_+, l_-) = i^{l_+ - l_-} e^{i[\delta_{l_-}(p_-) - \delta_{l_+}(p_+)]}.$$

In practice, we use the Gamow form of the correlation, Eq. (2).

The positronium formation cross section can also be written in a form that conveniently displays its angular dependence,

$$\frac{d\sigma}{d\Omega_{\text{Ps}}} = \frac{1}{(2\pi)^2} \left[\frac{E_i}{p_i} \right] \left[\frac{p_+ E_+}{2} \right] |\psi_{\text{Ps}}(0)|^2 \frac{1}{2} |M_{\text{Ps}}|^2, \quad (\text{B10})$$

where

$$\begin{aligned} |M_{\text{Ps}}|^2 = & \sum_{S, P, Q} (-1)^Q \frac{2Q+1}{4\pi} \sum_{\substack{\{\kappa\}, \lambda, J, \\ \{\kappa'\}, \lambda', J', \\ L, L', R}} (-1)^\lambda \phi_{l_i, l_+, l_-} \mathcal{C}_{\kappa L S J P Q} R_{\lambda J \kappa} \hat{l}_+ \hat{l}_- \hat{l}_i \langle l_- 0; l_+ 0 | L 0 \rangle \\ & \times (-1)^{\lambda'} \phi_{l_i', l_+', l_-'}^* \mathcal{C}_{\kappa' L' S' J' P' Q'} R_{\lambda' J' \kappa'}^* \hat{l}_+ \hat{l}_- \hat{l}_i' \langle l_- 0; l_+ 0 | L' 0 \rangle \\ & \times \left[\langle l_i 0; l_i' 0 | R 0 \rangle \langle L 0; L' 0 | R 0 \rangle \begin{Bmatrix} L & L' & R \\ l_i' & l_i & Q \end{Bmatrix} \frac{P_R(\cos\theta)}{4\pi} \right], \end{aligned} \quad (\text{B11})$$

with

$$\phi_{l_i, l_+, l_-} = (i)^{l_+ - l_i - l_-} e^{i[\delta_{l_-}(p_-) - \delta_{l_+}(p_+) - \delta_{l_i}(p_i)]}.$$

Here θ is the angle between the outgoing positronium and the incident positron. Angle integration over θ is done simply by taking only the $R=0$ term in Eq. (B11).

*Present address: TRIUMF, 4004 Wesbrook Mall, Vancouver, British Columbia, Canada V6T 2A3.

†Present address: Center for Theoretical Physics, Massachusetts Institute of Technology (Room 6-310), Cambridge, MA 02139.

‡Present address: Department of Physics, Indiana University, Bloomington, IN 47405.

¹J. Schweppe *et al.*, Phys. Rev. Lett. **51**, 2261 (1983); M. Clemente *et al.*, Phys. Lett. **137B**, 41 (1984); T. Cowan *et al.*, Phys. Rev. Lett. **54**, 1761 (1985); H. Tsertos *et al.*, Phys. Lett. **162B**, 273 (1985); T. Cowan *et al.*, Phys. Rev. Lett. **56**, 444 (1986); P. Kienle, in *Progress in Particle and Nuclear Physics*, edited by A. Faessler (Pergamon, New York, 1985), Vol. 15, p. 77; T. Cowan and J. S. Greenberg, Yale University Report No. 3074-927, 1986 (unpublished).

²For example, A. Schäfer *et al.*, J. Phys. G **11**, L69 (1985); A. B. Balentekin, C. Bottcher, M. R. Strayer, and S. J. Lee, Phys. Rev. Lett. **55**, 461 (1985); C. Y. Wong, *ibid.* **56**, 1047 (1986); B. Müller, J. Reinhardt, W. Greiner, and A. Schäfer, J. Phys.

G **12**, L109 (1986); C. Y. Wong and R. L. Becker, Phys. Lett. **B 182**, 251 (1986).

³J. Rafelski, B. Müller, and W. Greiner, Z. Phys. A **285**, 49 (1987); J. Reinhardt, U. Müller, B. Müller, and W. Greiner, *ibid.* **303**, 173 (1981).

⁴K. A. Erb, I. Y. Lee, and W. T. Milner, Phys. Lett. **B 181**, 52 (1986).

⁵The existence of these peaks has not been established without doubt. Some recent experiments have yielded contradictory results. See, for example, R. Peckhaus, W. Elze, T. Happ, and T. Dresel (unpublished); K. Maier *et al.* (unpublished); M. Sakai *et al.*, Institute for Nuclear Study (Tokyo) Report No. INS-Rep-632, 1987 (unpublished).

⁶H. J. Bhabha, Proc. R. Soc. London, Ser. A **154**, 195 (1935).

⁷J. D. Bjorken and S. D. Drell, *Relativistic Quantum Mechanics* (McGraw-Hill, New York, 1964).

⁸P. Gombas, *Die Statische Theorie des Atoms* (Springer, Vienna, 1949).